MARTIN MARIETTA ENERGY SYSTEMS LIBRARIES

3 4456 0364200 2

CENTRAL RESEARCH LIBRARY
DOCUMENT COLLECTION

ORNL-3025
UC-34 - Physics and Mathematics

RAINBOW SCATTERING ANALYSIS OF RECENT HEAVY ION DATA

M. V. Goldman

CENTRAL R
DOCUME
LIBRARY
DO NOT TRANSF
If you wish s
document, sen
and the libra

OAK RIDGE NATIONAL LABORATORY
operated by
UNION CARBIDE CORPORATION
for the
U.S. ATOMIC ENERGY COMMISSION

Printed in USA. Price 75 cents. Available from the
Office of Technical Services
Department of Commerce
Washington 25, D.C.

LEGAL NOTICE

This report was prepared as an account of Government sponsored work. Neither the United States, nor the Commission, nor any person acting on behalf of the Commission:

A. Makes any warranty or representation, expressed or implied, with respect to the accuracy, completeness, or usefulness of the information contained in this report, or that the use of any information, apparatus, method, or process disclosed in this report may not infringe privately owned rights; or

B. Assumes any liabilities with respect to the use of, or for damages resulting from the use of any information, apparatus, method, or process disclosed in this report.

As used in the above, "person acting on behalf of the Commission" includes any employee or contractor of the Commission, or employee of such contractor, to the extent that such employee or contractor of the Commission, or employee of such contractor prepares, disseminates, or provides access to, any information pursuant to his employment or contract with the Commission, or his employment with such contractor.

ORNL 3025
Physics and Mathematics

Contract No. W-7405-eng-26

ELECTRONUCLEAR RESEARCH DIVISION

RAINBOW SCATTERING ANALYSIS OF RECENT HEAVY ION DATA

M. V. Goldman

DATE ISSUED

DEC 28 1960

OAK RIDGE NATIONAL LABORATORY
Oak Ridge, Tennessee
Operated by
UNION CARBIDE CORPORATION
for the
U.S. ATOMIC ENERGY COMMISSION

MARTIN MARIETTA ENERGY SYSTEMS LIBRARIES
3 4456 0364200 2

TABLE OF CONTENTS

Abstract 1

Theory 2

Method of Fitting 8

Best Fits to Experimental Data 9

Discussion 11

Appendix I: ΔR Redefined in Terms of Δ 14

Appendix II: Correction for Angular Variation in the Wheeler-Ford Expression for $\frac{\sigma}{\sigma_c}$ 15

Rainbow Scattering Analysis of Recent Heavy Ion Data

M. V. Goldman*

Oak Ridge National Laboratory

ABSTRACT

Heavy-ion elastic scattering cross sections recently obtained for C^{12}, N^{14}, O^{16} and Ne^{20} by Au^{197} and Bi^{209}, and scattering of C^{12} by Ni^{59}, Ag^{107}, In^{113}, and Ta^{181}, all at about 10 Mev/nucleon incident energy, are fitted by means of the semiclassical rainbow model of Ford and Wheeler. Values of r_o in very good agreement with the sharp cut-off model are found. The non-absorbing nuclear surface thickness of the rainbow model is found to be about 2 fermis, or 18% of the interaction radius, and shows little variation with either projectile or target mass for these data. Several aspects of the theory itself are examined.

---

*ORNL summer employee, now at Harvard University, Physics Department.

THEORY

When a light ray enters a spherical water droplet, is internally reflected once, and emerges, simple geometric optics predicts that the angle of deviation or scattering of the ray (θ) as a function of impact parameter ($\underline{b}$) will have a minimum at some $\underline{b}_o$ less than the radius of the droplet. Since the classical expression for the differential scattering cross section contains a $\frac{d\theta}{d\underline{b}}$ in the denominator, a singularity in intensity arises at the angle of minimum deviation, $\theta(\underline{b}_o)$, where $\frac{d\theta}{d\underline{b}_o} = 0$. We observe this phenomenon in nature in the appearance of rainbows*. Here $\theta(\underline{b}_o)$ is the "rainbow angle" and we will henceforth denote such extrema by θ_r.

No ray can be deflected by an angle less than θ_r, so the cross section computed from geometric optics will obviously be zero at angles smaller than θ_r (dark side of the rainbow). A more sophisticated treatment, using wave optics to account for diffraction effects, would yield a large but finite oscillating intensity on the bright side and a greater than exponential fall-off on the dark side.

All this has an analogue in nuclear physics according to a recent semiclassical scattering theory developed by Ford and Wheeler[1], which they apply to the scattering of α-particles by

---

*The variety of colors corresponds to the slightly different angles of minimum deviation for the various wave lengths present in white light.

[1] K. W. Ford and J. A. Wheeler, Annals of Physics 7, 259 (1959)

heavy nuclei. They define the deflection function Θ to be the scattering angle θ as a function of angular momentum ℓ for a repulsive force, and the negative of θ for an attractive force. The qualitative behavior of the deflection function for scattering of nuclei by nuclei is clear if one ignores absorption (see Fig. 1). For large ℓ and a fixed energy E, Θ will be close to zero. As ℓ decreases, will monotonically increase, due to the Coulomb repulsion, until the short-range attractive nuclear force comes into play. Here Θ will begin to decrease as ℓ decreases, becoming negative as the nuclear force dominates, and approaching $-\infty$, which corresponds to spiralling of the projectile around the target.

As in the scattering of light by water droplets, the deflection function has an extremum which implies an infinite classical cross section at the rainbow angle θ_r. Now, however, it is a maximum, and the high-angle side of θ_r is the black side (zero cross section). This classical behavior of the cross section would be correct if the scattering of a beam of nuclei actually involved well-defined paths. But quantum-mechanically, the definition of the path is limited by the uncertainty principle, and wave ideas must be introduced. Just as wave optics accounted for diffraction effects in the scattering of light by water droplets, so wave mechanics can lead to a semiclassical cross section which accounts for diffraction effects in nuclear scattering and predicts a similar cross section behavior (i.e. oscillating on the bright side and a greater than exponential fall-off on the dark side of θ_r). Ford and Wheeler follow a semiclassical partial wave analysis

as outlined below:

The quantum expression for scattering is,

$$\sigma = \left| f(\theta) \right|^2, \tag{1}$$

where the amplitude $f(\theta)$ is:

$$f(\theta) = \frac{1}{2ik} \sum_{\ell=0}^{\infty} (2\ell + 1)(e^{2i\delta_\ell} - 1) P_\ell (\cos \theta). \tag{2}$$

Here δ_ℓ is the phase shift of the ℓth partial wave. Table 1 gives the approximations valid under a semiclassical analysis and the conditions for validity.

Table 1. Approximations for the Ford-Wheeler semiclassical analysis.

Approximation	Conditions for validity (Necessary, not suff.)
1. The phase shifts are evaluated by the JWKB method.	1. (a) δ_ℓ large (b) Slowly varying potential.
2. The Legendre polynomial is replaced by its asymptotic form.	2. (a) Large ℓ (b) $\sin \theta \geq \frac{1}{\ell}$
3. The summation of Eq. (2) is replaced by an integral.	3. Large $\Delta \ell$ (many partial waves contribute to the scattering).

These approximations convert the expression for the scattering amplitude, Eq. 2, into the semiclassical form:

$$f_{s.c.} = -\frac{1}{k(2\pi \sin\theta)^{1/2}} \int_0^\infty (\ell + 1/2)^{1/2}(e^{i\phi_+} - e^{i\phi_-})d\ell , \qquad (3)$$

where,

$$\phi_\pm = 2\,\mathcal{S}_\ell \pm(\ell + 1/2)\,\theta \pm \pi/4. \qquad (4)$$

The main contribution to the integral comes from the region where either exponential varies slowly. This will be in the vicinity of the ℓ -value of stationary phase (s.p.) at which $\phi_\pm$ is not changing with respect to ℓ :

$$\left.\frac{d\phi_\pm}{d\ell}\right|_{\ell_{s.p.}} = 0 \qquad (5)$$

Differentiating Eq. (4) and setting equal to zero, therefore, gives the condition:

$$\left.\frac{d\mathcal{S}_\ell}{d\ell}\right|_{\ell_{s.p.}} = \frac{1}{2}\,\Theta\,(\ell_{s.p.}) \qquad (6)$$

Relation (6) determines the phase shifts if $\Theta\,(\ell)$ is known. Hence, one need only know the classical deflection function to evaluate the semiclassical cross section, which will be the square of the absolute value of the right-hand side of Eq. (3). In practice, of course, the situation is reversed. In many cases the cross section has been measured experimentally and one wishes to know the shape of the deflection function in Fig. 1 around the neighborhood of ℓ_r. It is therefore necessary to somehow parametrize $\theta(\ell - \ell_r)$ and fit the resulting expression for $\sigma_{s.c.}$ to the experimental cross section, thereby determining the parameters and, hence, the shape.

As a first approximation, Ford and Wheeler assume a parabolic deflection function

$$\Theta(\ell) = \theta_r - q\,(\ell - \ell_r)^2. \tag{7}$$

This leads to the cross section

$$\sigma = \frac{1}{k^2}\,(\ell_r + 1/2)\left(\frac{2\pi}{\sin\theta}\right)\left|\, q^{-2/3} \,\right| \mathrm{Ai}^2(x). \tag{8}$$

Ai(x) is the Airy integral,

$$\mathrm{Ai}(x) = \frac{1}{2\pi}\int_{-\infty}^{+\infty} \exp(ixu + 1/3\, iu^3)\,du,$$

and x is defined by the formula

$$x = q^{-1/3}(\theta_r - \theta). \tag{9}$$

A more convenient expression in the neighborhood of the rainbow angle is the ratio of σ/σ_c, where σ_c is the value at θ_r of the Coulomb scattering cross section

$$\frac{\sigma}{\sigma_c} = \frac{4\pi}{\eta}\,(q^{-1/3}\sin\theta_r/2)^2\mathrm{Ai}^2(x), \tag{10}$$

$$\eta = \frac{Z_1 Z_2 e^2}{\hbar v}$$

With a proper choice of the parameters q and θ_r, Eq. (10) can be made to agree quite well with experimental σ/σ_c, around θ_r, provided η is sufficiently greater than one. The parameters θ_r and q can be related to other quantities of more direct physical significance, such as an interaction radius R and nuclear surface thickness ΔR.

If, as we have reason to believe, the nuclear force begins to dominate the Coulomb force quite rapidly when the nuclei are close, then, at θ_r the value of ℓ derived from the Coulomb deflection function will be reasonably close to ℓ_r (derived from the actual deflection function) and we may use the Coulomb expression for the distance of closest approach as a function of scattering angle:

$$R = \frac{\eta}{k}(1 + \csc \theta_r/2). \tag{11}$$

Thus, the rainbow angle gives us an interaction radius directly. The nuclear radius parameter r_o may be found in the usual way by dividing by $(A_1^{1/3} + A_2^{1/3})$.

In the rainbow model, absorption is ignored for ℓ-values greater than ℓ_s, where spiralling begins. Then the scattering for ℓ-values between ℓ_s and ℓ_r may be regarded as due to a non-absorbing refractive surface layer of thickness related to $(\ell_r - \ell_s)$. Since the actual ℓ_s is not known, Ford and Wheeler take as $\Delta\ell$ the distance between the axis of the approximating parabola (ℓ_r) and its intersection with the ℓ-axis at ℓ_o. Since $\Theta = \theta_r - q(\ell_o - \ell_r)^2$, we have

$$\Delta\ell = |\ell_o - \ell_r| = (\theta_r/q)^{1/2}. \tag{12}$$

The value of $\Delta\ell$ depends on the agreement between $\theta_r - q(\ell - \ell_r)^2$ and the actual deflection not only in the neighborhood of θ_r, but also at $\theta=0$. We shall return to this point later. A surface thickness ΔR is obtained from $\Delta\ell$ by dividing by the wave number k. In Appendix I of the present paper, an alternative method of defining ΔR is presented.

METHOD OF FITTING

Expression (10) was fitted to the experimental σ/σ_c vs θ mainly by a graphical method. Some fits were also made to rainbow model curves calculated on the IBM 704, but the hand technique was found preferable in that it allowed more control at less expense and was only slightly slower. The graphical method is as follows:

We rewrite expression (10) as

$$\sigma/\sigma_c = \alpha Ai^2(x), \tag{13}$$

where α is the constant $4\pi/\eta\ (q^{-1/3} \sin \theta_r/2)^2$ and $x = q^{-1/3}(\theta_r - \theta)$. The two independent parameters to be varied are taken as θ_r and α. On a large piece of graph paper, x is put on the abscissa, and both Ai^2 and θ are put on the ordinate, Fig. 2. The function $Ai^2(x)$ is actually plotted on the graph, while the straight line representing $x = q^{-1/3}(\theta_r - \theta)$ is scored on a length of plexiglass which is laid over the graph in a position determined by the choice of parameters. In this manner, the variation of the two parameters is accomplished by taking advantage of the two degrees of freedom of the straight line. After α and θ_r are chosen and $q^{-1/3}$ computed, the line is easily positioned, since the θ intercept is just θ_r, and the x-intercept is $-0.01745\ q^{-1/3}\ \theta_r$, or, alternatively, the slope $dx/d\theta$ is $0.01745\ q^{-1/3}$. When the line is fixed, one reads from θ to the straight line, to the plotted curve, to the value of $Ai^2(x)$ corresponding to that θ (see above diagram). The value of x need not even be read off. One then multiplies $Ai^2(x)$ by the scale factor α which may be kept as constant multiplier on a desk calculator. It

quickly becomes apparent how to control the shape of σ/σ_c by utilizing different portions of the $Ai^2(x)$ curve (determined by the slope and intercept of the straight line) and by changing the multiplicative factor π. Two rough but valuable rules of thumb are as follows:

A. To increase (or decrease) the downward slope of the lower portion of σ/σ_c, increase (or decrease) α.

B. To move the lower part of σ/σ_c to the left (or right), decrease (or increase) θ_r.

One can come close to a fit even at first try, by choosing for θ_r an angle corresponding on the experimental curve to a σ/σ_c between 0.3 and 0.5 and an α equal to that value of σ/σ_c divided by 0.126*. Then α and θ_r are adjusted to obtain a best fit.

BEST FITS TO EXPERIMENTAL DATA

The data fitted in this paper were recently presented at the Second Conference on Reactions Between Complex Nuclei at Gatlinburg, Tennessee, May 2-4, 1960. Kerlee, Reynolds, and Goldberg[2] have investigated the elastic scattering of C^{12}, N^{14}, O^{16} and Ne^{20} by Au^{197} and Bi^{209} at energies of 10.4 Mev (lab) per nucleon, while Alster and Conzett[3] have studied elastic scattering of C^{12} by Ni^{59}, Ag^{107}, In^{113} and Ta^{181} at 124.5 Mev (lab). The experimental σ/σ_c curves of both groups provide excellent data for examination of the dependence of r_o and ΔR of the rainbow model on the masses of targets and projectiles.

---

*At $\theta = \theta_r$, $x = 0$, and $Ai^2(0) = 0.126$. Hence, choosing $\alpha = (\sigma/\sigma_c)_{exp}/0.126$ will always put the rainbow angle right on the experimental curve.

In the process of fitting, it soon became apparent that different fits were possible over different regions. There is a theoretical reason, however, for expecting $(\sigma/\sigma_c)_{theor.}$ to be a better fit to $(\sigma/\sigma_c)_{exp.}$ on the dark (high angle) side of the rainbow angle than on the bright (low angle) side. On the bright side, contributions to $(\sigma/\sigma_c)_{theor.}$ come from the low-ℓ and high-ℓ branches of the deflection function. If the nuclear absorption is appreciable, however, waves with low ℓ-values will traverse much of the nuclear interior and will, therefore, be rapidly damped out, leaving only the contribution of waves which miss the nucleus and give rise to ordinary Coulomb scattering. This should damp the bright side oscillations predicted by the rainbow theory, since the theory does not take absorption into account. The dark side behavior remains unaffected.

In Fig. 3 are seen two different possible fits to experimental data. The fit on the right was chosen as best, although the limits of accuracy given below on the parameters r_o and ΔR are such as to permit the left hand fit also. Figure 4 shows how relatively insensitive a fit is to ΔR. In the particular case shown, acceptable fits are obtained with ΔR's ranging from 1.7 to 2.4 fermis. Figure 5 shows the effect on a best fit of a variation of r_o by about ±1% and a variation of ΔR by about 12%. Variation of the parameters by more than these amounts produces unacceptable fits, therefore, they were taken as the limits of accuracy of the determination of r_o and ΔR. The values of r_o and ΔR were also varied over a much larger range, but fits were found to be possible only in the neighborhood defined by the above limits; this neighborhood is unique. In Figs. 6 and 7

are shown the rainbow fits to all of the data of Alster and Conzett[3] and part of the data of Kerlee, Reynolds and Goldberg[2]. The data of the former lent itself to fits over wider angular ranges since Alster and Conzett examine σ/σ_c as low as 0.01, while Kerlee, Reynolds and Goldberg only go down to 0.1.

DISCUSSION

In Tables 2 and 3 all relevant parameters of the fits are summarized. Table 2 is ordered according to increasing target mass with C^{12} as the projectile. The results of the rainbow fit of Halbert and Zucker[4] to scattering of N^{14} by Al^{27} at 27.3 Mev are inserted at the head of the table for comparison. Table 3 is ordered according to increasing projectile mass with Au^{197} and Bi^{209} as targets. With E_{lab} in Mev and all masses in amu other quantities in the table are calculated via the following formulas:

---

[2] D. D. Kerlee, H. L. Reynolds and E. Goldberg, Reactions Between Complex Nuclei, John Wiley and Sons, Inc. (1960), p. 167.

[3] J. Alster and H. E. Conzett, Reactions Between Complex Nuclei, John Wiley and Sons, Inc. (1960), p. 175.

[4] M. L. Halbert and A. Zucker, Nuclear Physics 16, 158 (1960).

$$\eta = 0.1574 \frac{Z_1 Z_2}{(E_{lab}/M_1)^{1/2}}$$

$$k = 0.2187 \frac{M_2}{M_1 + M_2} (M_1 E_{lab})^{1/2}$$

$$\ell_r = \eta \cot \theta_r/2 - 1/2 \qquad \text{(semiclassical Coulomb)}$$

$$\Delta S_\ell = 0.01745\, \Delta\ell\, (\theta_r/2) \qquad \text{(from Eq. 6).}$$

Also used are Eqs. (11) and (12) for ΔR and R.

In most cases, ℓ_r, $\Delta\ell$, and ΔS_ℓ are found to be sufficiently greater than unity to validate a semiclassical analysis (compare with Table 1).

The values obtained for r_o from rainbow angles ranging from 16° to 40° are all remarkably consistent and close to r_o's obtained from the Blair sharp-cutoff model[5]. Kerlee, Reynolds and Goldberg[2] obtain agreement with the sharp cutoff model by using $r_o \approx 1.46$ fermis (see Table 4). These fits exhibit some diffraction structure and are generally much better at the lower angles, while the rainbow fits fall off smoothly and are better at the higher angles. It is striking that similar r_o's are obtained not only from very different models, but also from completely different portions of the experimental data.

Of greater interest perhaps is the number, $\Delta\ell$, or refracted but unabsorbed partial waves of ℓ-value lower than ℓ_r, or the "surface thickness" ΔR derived from $\Delta\ell$. Most conspicuous are the rather large values obtained for $\Delta\ell$ and ΔR from the rainbow

---

[5] J. S. Blair, Phys. Rev. 95, 1218 (1954).

fits made in this paper. For $\ell_r = 65$ we find $\Delta\ell$ to be about 16 partial waves, which is large compared with Alster and Conzett's "fuzzed"* fits to their data which yield $\Delta\ell$'s of 2 and 3 around $\ell_o = 62$. Using $\Delta R = \Delta\ell/k$, we derive nuclear surface thicknesses of about 2 fermis. The fits are not accurate enough to obtain any information about the dependence of ΔR on either target or projectile mass and structure. The only significant difference is in the $Al^{27}(N^{14}, N^{14})Al^{27}$ scattering data of Halbert and Zucker, for which $\Delta R = 0.84$ fermis. This, however, is the only low-energy rainbow fit (aside from α-particles), and it is over a very different angular range (91° to 131°).

In the following two appendices, we consider the consequences of making more precise two approximations of the Ford and Wheeler treatment.

---

*The "fuzzed" model is similar to the Blair model except that instead of a sharp cutoff for a particular ℓ-value of the partial wave expansion, there is a gradual decrease of the amplitude of the ℓth wave with ℓ according to the arbitrary rounding function $\left\{1 + \exp\left[-(\ell - \ell')/\Delta\ell\right]\right\}^{-1}$ introduced by McIntyre, Baker and Wang[6].

[6] J. A. McIntyre, S. D. Baker, and K. H. Wang, Phys. Rev. (In press).

APPENDIX I: ΔR Redefined in Terms of $\Delta \ell$

The measure of non-absorbing surface thickness used by Ford and Wheeler is $\Delta R = \Delta \ell / k$. Strictly speaking, however, this gives one an increment in impact parameter, Δb, rather than surface thickness since k is the wave number at infinity. The initial angular momentum is $\ell = bk$, which equals $R\ k_R$ at perihelion (k_R is the wave number at perihelion). Only if $k \simeq k_R$ will $\ell / k = R$, or $\Delta \ell / k = \Delta R$; this is satisfied only if the projectile slows down only slightly in the Coulomb field. It seems reasonable to divide by k_R directly, where k_R is taken as ℓ_r / R. We then define ΔR^* by the equation,

$$\Delta R^* = \Delta \ell / k_R = (\Delta \ell / \ell_r) R \qquad (14)$$

(ℓ_r and R are found from the rainbow angle via the Coulomb expressions $\ell_r = \eta \cot \theta_r/2 - 1/2$, $R = \eta / k\,(1 + \csc \theta_r/2)$. In Table 4 the surface thickness ΔR^* is compared with Ford and Wheeler's ΔR. Also compared are the ratios of surface thickness to interaction radius. The ΔR^* for the low energy aluminum scattering is more in line with the other ΔR^*'s, now appearing relatively larger instead of smaller.

APPENDIX II: Correction for Angular Variation in the Ford-Wheeler Expression for (σ/σ_c)

The scattering cross section for a Coulomb force may be written as:

$$\sigma_c = \frac{1}{4}\left(\frac{\eta}{k}\right)^2 \frac{1}{\sin^4\theta/2} = \frac{1}{2}\left(\frac{\eta}{k}\right)^2 \frac{\cot\theta/2}{\sin\theta} \frac{1}{\sin^2\theta/2} \tag{15}$$

If one inserts the semiclassical Coulomb relation between angular momentum and scattering angle, $(\ell + 1/2) = \eta \cot\theta/2$, the Coulomb cross section may be rewritten as,

$$\sigma_c = \frac{1}{2}\frac{\eta}{k^2}\frac{(\ell + 1/2)}{\sin\theta}\frac{1}{\sin^2\theta/2}\,. \tag{16}$$

Ford and Wheeler derive the rainbow scattering cross section,

$$\sigma = \frac{1}{k^2}(\ell_r + 1/2)\left(\frac{2\pi}{\sin\theta}\right) q^{-2/3}\mathrm{Ai}^2(x)\,. \tag{17}$$

Their expression for σ/σ_c is obtained by freezing the $\sin\theta$ in the denominator of σ at $\sin\theta_r$ and dividing by the value of the Coulomb cross section at θ_r:

$$\sigma/\sigma_c = \frac{\frac{1}{k^2}(\ell_r + 1/2)\frac{2\pi}{\sin\theta_r} q^{-2/3}\mathrm{Ai}^2(x)}{1/2\,\frac{\eta}{k^2}\frac{(\ell_r + 1/2)}{\sin\theta_r}\frac{1}{\sin^2\theta/2}} \tag{18}$$

$$= \frac{4\pi}{\eta}\left(\sin\theta_r/2\, q^{-1/3}\right)^2 \mathrm{Ai}^2(x).$$

This expression is valid only in a small region about the rainbow angle. To take the angular variation into account we must divide the σ of (17) (with $\ell_r + 1/2 = \eta \cot\theta_r/2$) directly by the σ_c of (15), obtaining,

$$\left[\frac{\sigma}{\sigma_c}\right]_\theta = \frac{4\pi}{\eta}\frac{\cot\theta_r/2}{\cot\theta/2}\left(\sin\theta/2\, q^{-1/3}\right)^2 Ai^2(x). \tag{19}$$

In terms of the Ford-Wheeler expression (18), $\left[\frac{\sigma}{\sigma_c}\right]_\theta$ may be rewritten as,

$$\left[\frac{\sigma}{\sigma_c}\right]_\theta = \gamma(\theta)\,\sigma/\sigma_c, \text{ where } \gamma(\theta) = \frac{\cot\theta_r/2}{\cot\theta/2}\;\frac{\sin\theta/2}{\sin\theta_r/2}. \tag{20}$$

At each angle of one of the fitted σ/σ_c curves we computed the correction factor γ and the value of $\left[\frac{\sigma}{\sigma_c}\right]_\theta$. The result is shown in Fig. 8. The previously successful parameters r_o and ΔR no longer provide a good fit. The best fit with revised parameters of $\left[\frac{\sigma}{\sigma_c}\right]_\theta$ to the experimental data is also shown. Both r_o and ΔR for this fit are slightly higher. The parameters are compared in Table 6.

UNCLASSIFIED
ORNL-LR-DWG 52418

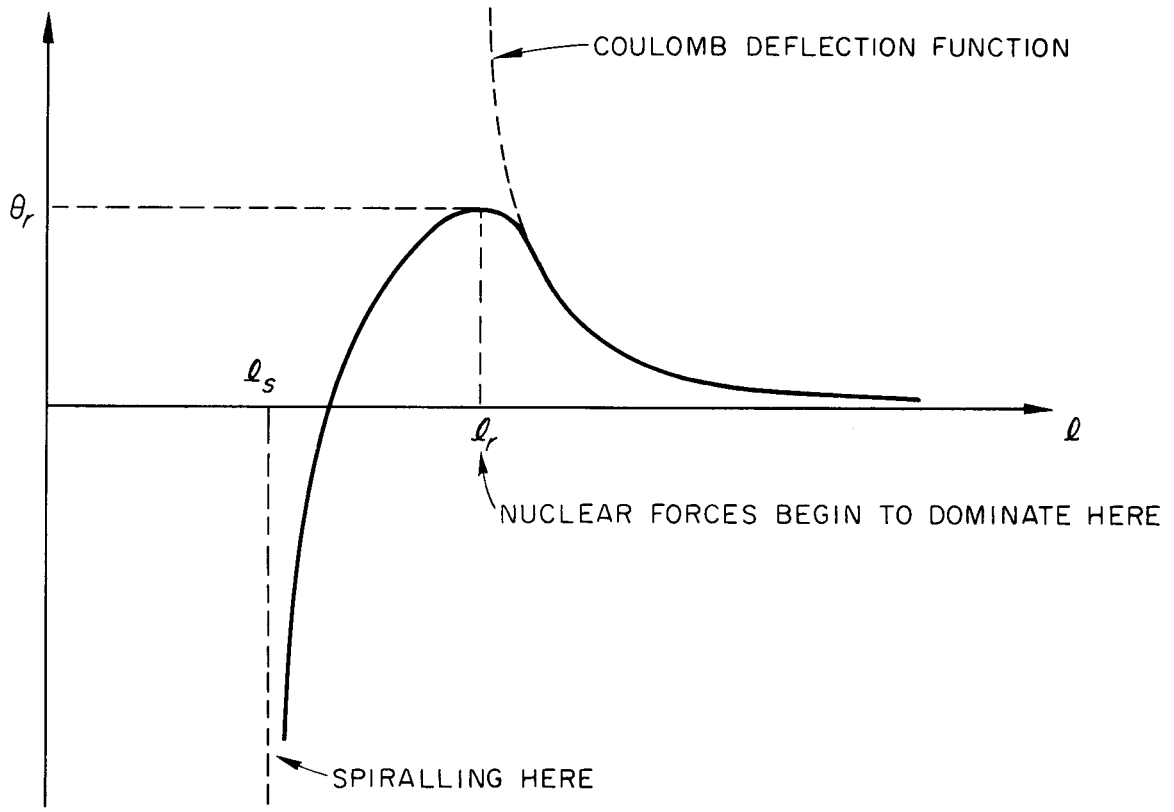

Fig. 1. Classical Deflection Function vs Angular Momentum, Where Absorption is Ignored. The characteristic features of rainbow angle and spiral scattering are depicted.

UNCLASSIFIED
ORNL-LR-DWG 52419

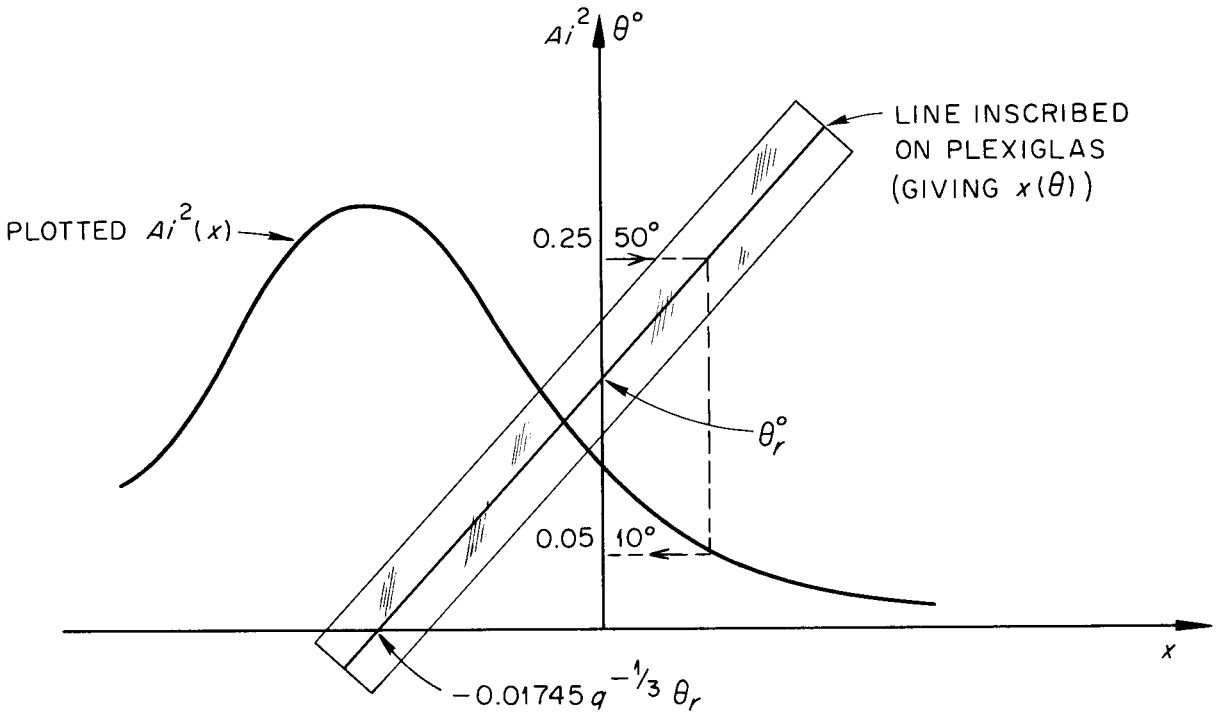

Fig. 2. Graphical Technique for Fitting Rainbow Model σ/σ_c Curves. The square of the Airy function is actually plotted, while the straight line representing $x = q^{-1/3}\ (\theta_r - \theta)$ is inscribed on a length of Plexiglass.

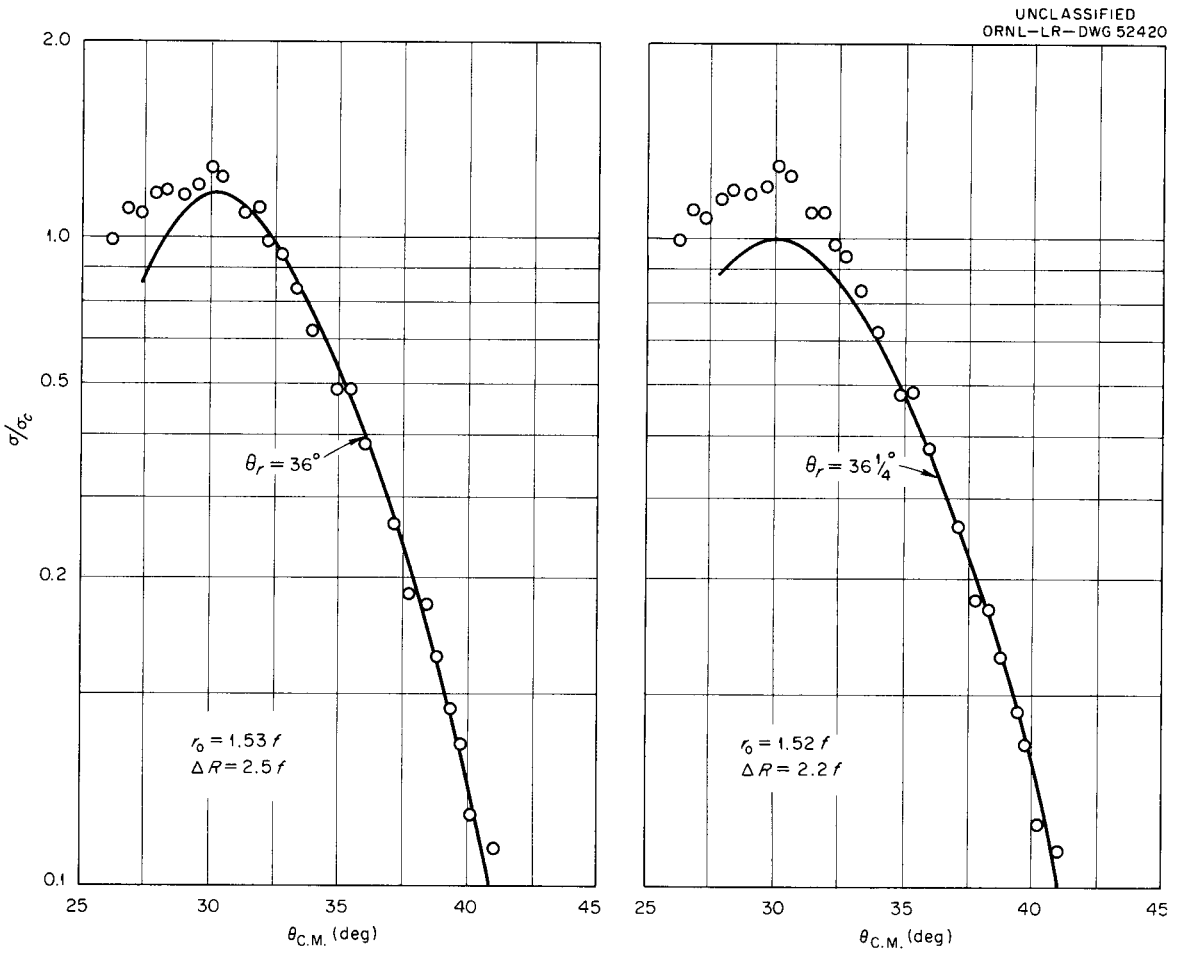

Fig. 3. Rainbow Fits to the 164.1-Mev (lab), $Au^{197}(O^{16}, O^{16})Au^{197}$ Cross-Sections of Kerlee, Reynolds and Goldberg.[2] The curve on the right was regarded as the best fit.

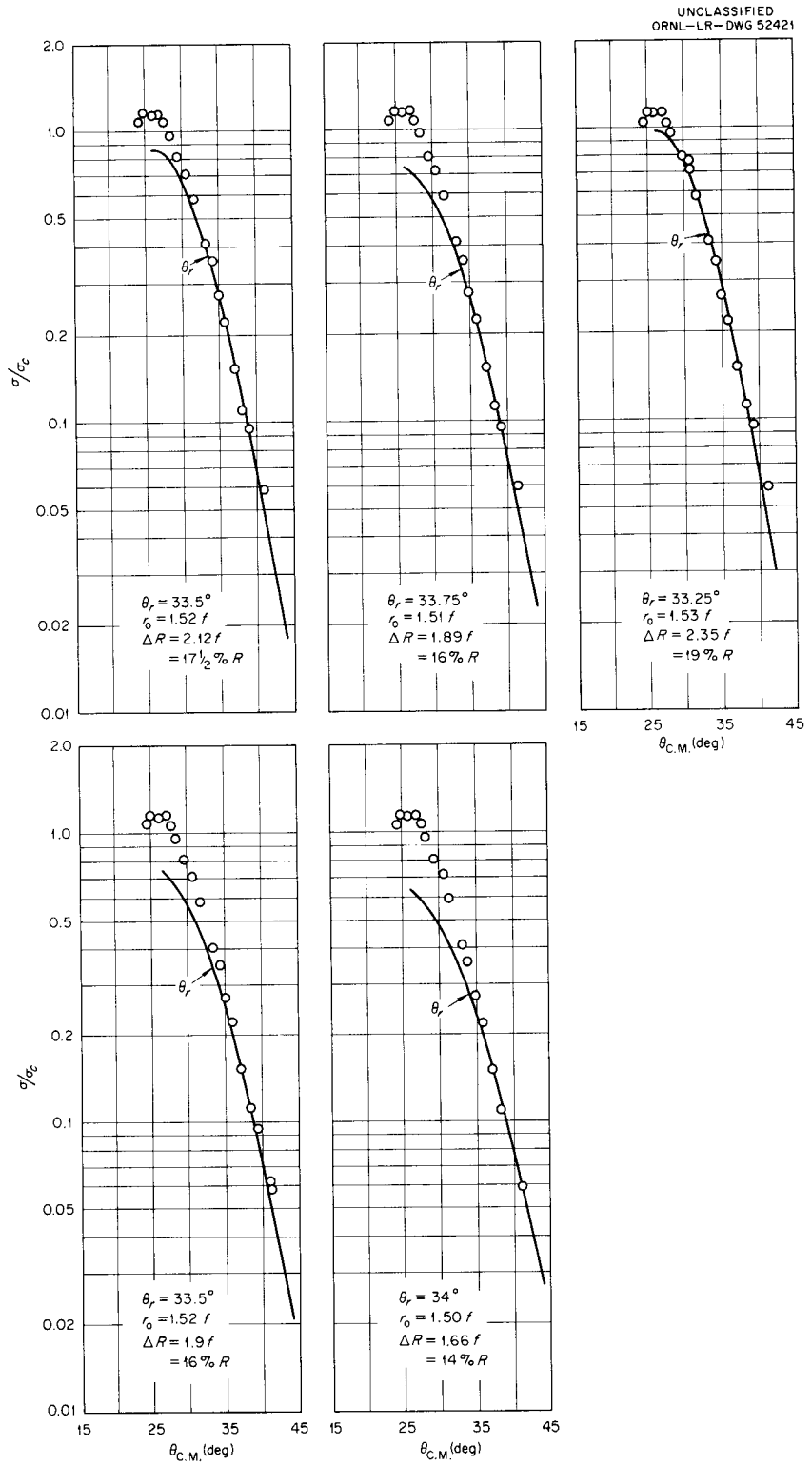

Fig. 4. Illustration of Good Rainbow Fits Obtained with Widely Varying ΔR's ($1.66 \leq \Delta R \leq 2.35$). Curve 1 was regarded as the best fit. The data was from Alster and Conzett[3] for $Ta^{181}(C^{12}, C^{12})Ta^{181}$ at E_{lab} = 1.24.5 Mev.

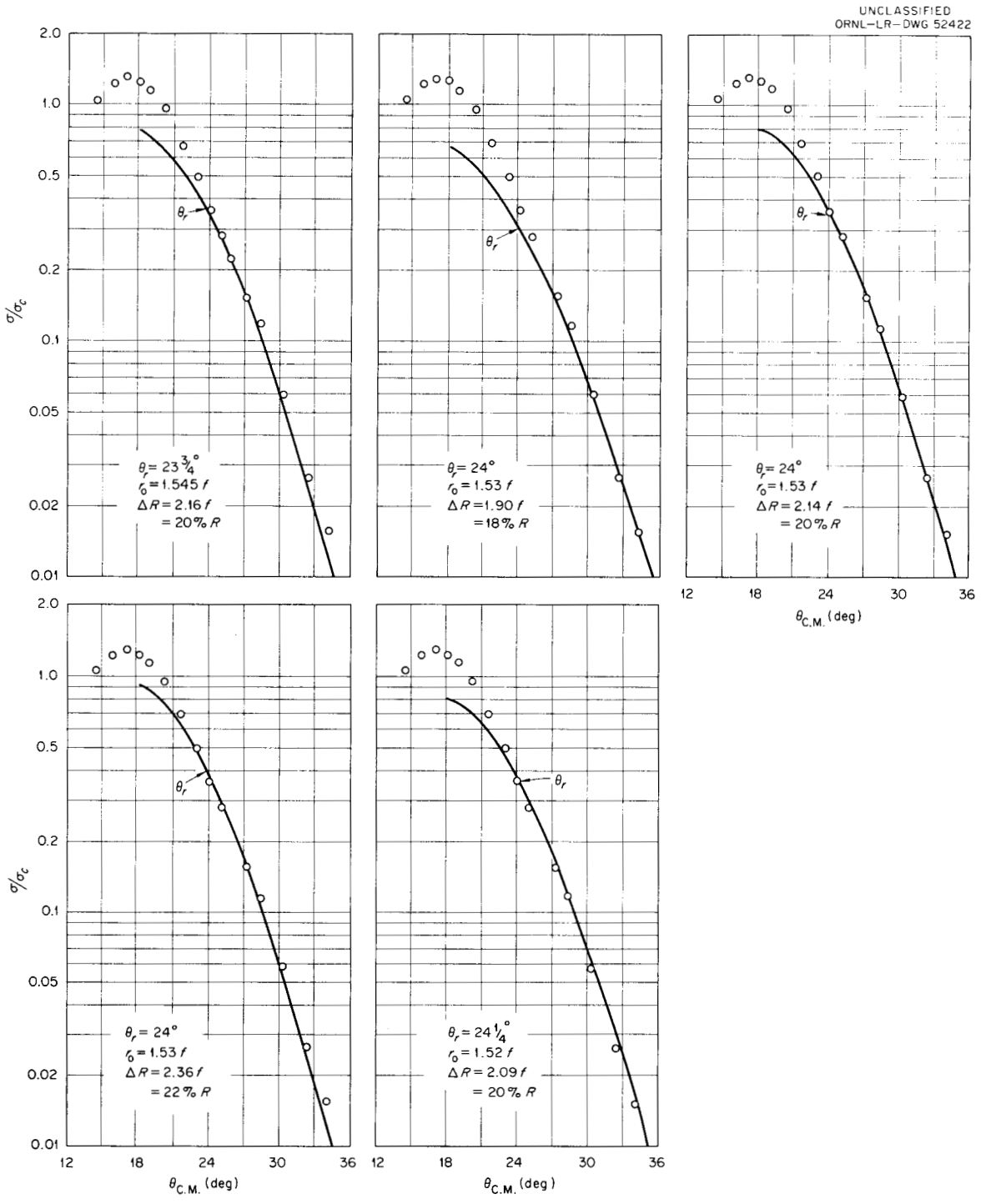

Fig. 5. Limits of Accuracy of Determination of the Parameters r_0 and ΔR in a Rainbow Fit. Variation of r_0 by more than about ±1% or ΔR by more than about ±12% produces a visibly poorer fit. The data is that of Alster and Conzett[3] for $In^{113}(C^{12},C^{12})In^{113}$ at E_{lab} = 124.5 Mev.

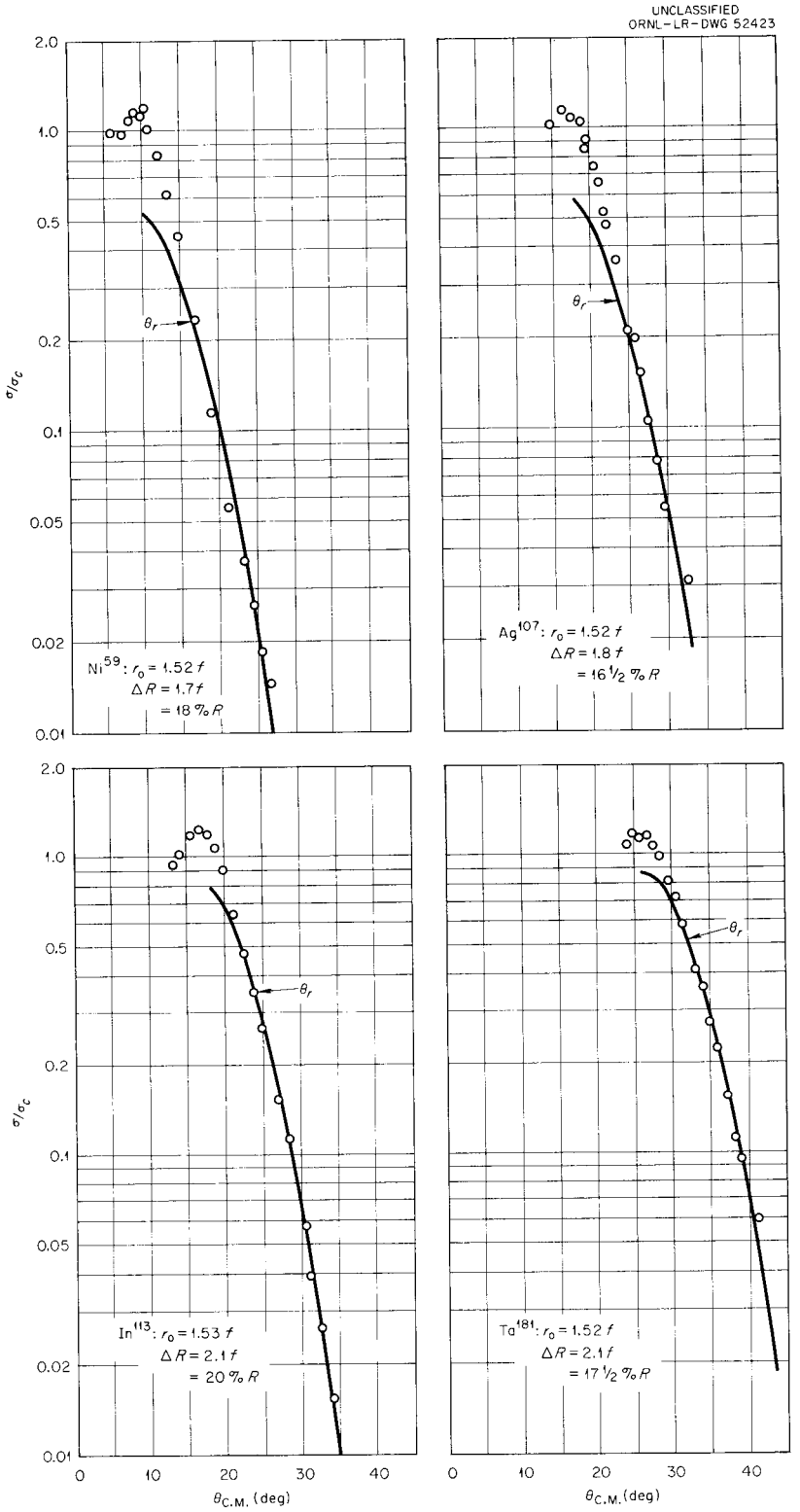

Fig. 6. Rainbow Fits for C^{12} Scattered from Various Targets at E_{lab} = 124.5 Mev. (Data of Alster and Conzett[3]). Values of r_0 and ΔR for each of the four targets are given.

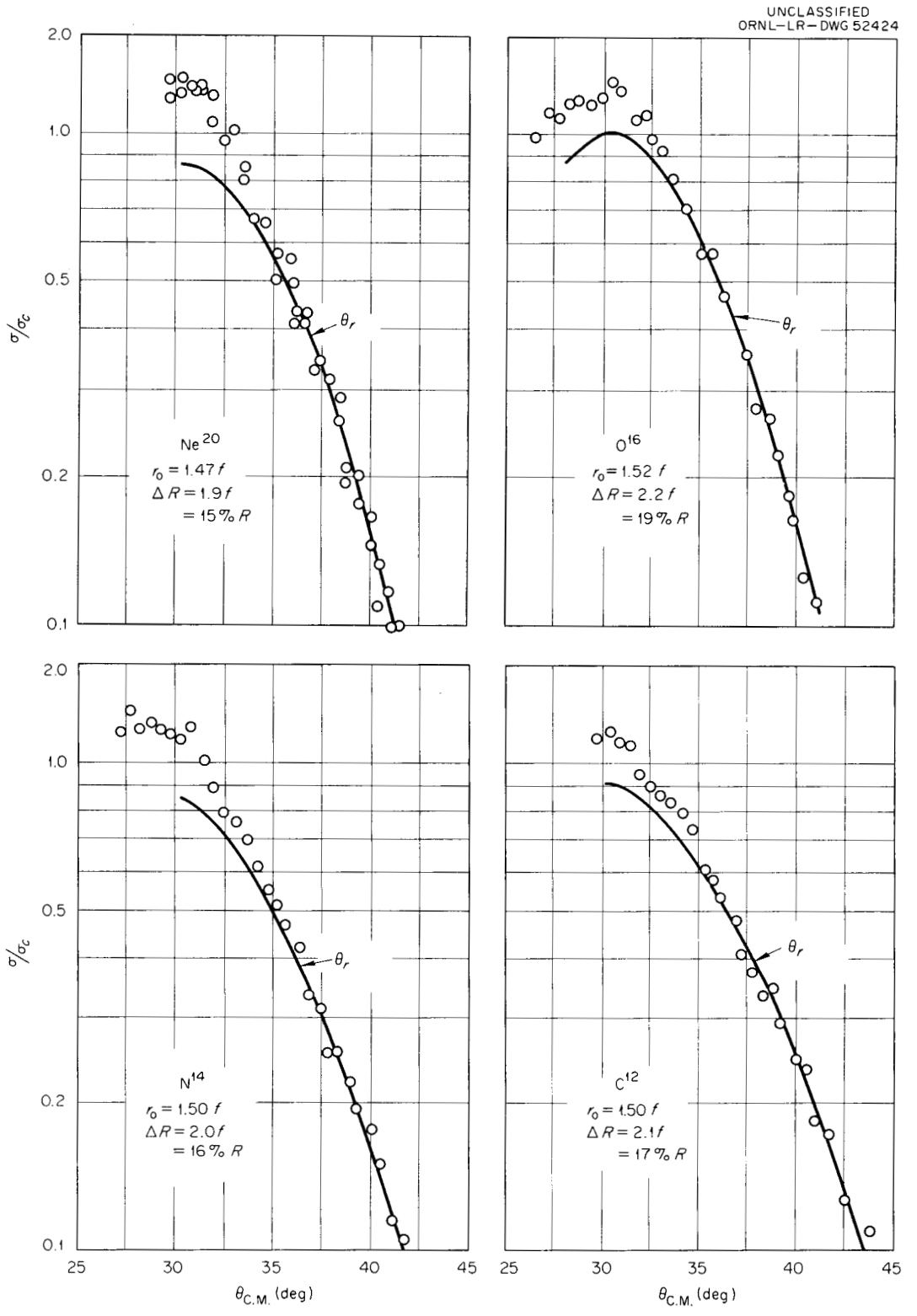

Fig. 7. Rainbow Fits for Various Projectiles Scattered from Au^{197} at ~10.4 Mev (lab) Energy Per Nucleon. (Data of Kerlee, Reynolds and Goldberg[2]). Values of R_0 and ΔR for each of the four projectiles are given.

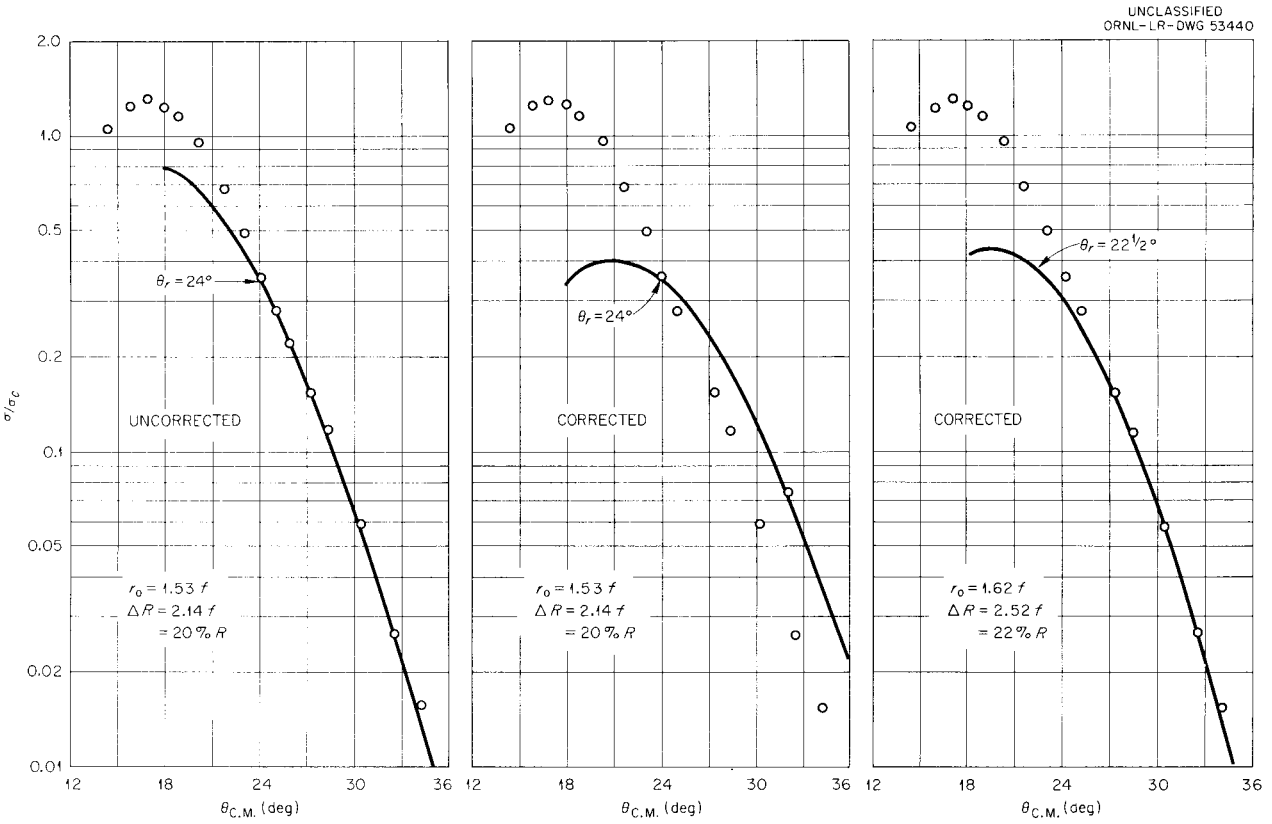

Fig. 8. Effect of Correcting for the Angular Variation of σ_c and $\sigma_{rainbow}$. Curve 1 was the best fit for the Ford-Wheeler expression for σ/σ_c. Curve 2 shows the effect of the correction for angular variation on this fit. Curve 3 shows the fit obtained with the angle-corrected expression and the new values of the parameters r_0 and ΔR.

Table 2. Rainbow scattering correlations.

Mass*					Fitted Region											
M_1	M_2	E_{lab}	η	k	θ	σ/σ_c	θ_r	r_o	R	ΔR	$\frac{\Delta R}{R}$	ℓ_r	$\Delta \ell$	$\Delta \delta_\ell$	Reference
14	27	27.3	10.3	2.8	91°-131°	.2-.01	94	1.60	8.6	.84	10%	9	2.4	2.0	4
12	59	124.5	8.2	7.0	16°-26°	.25-.01	16.25	1.52	9.4	1.7	18%	58	12.0	1.7	3
12	107	124.5	13.8	7.6	23.5°-32°	.25-.03	23.50	1.52	10.7	1.8	16.5%	64	14.0	2.9	3
12	113	124.5	14.4	7.7	24°-34°	.35-.01	24	1.53	10.9	2.1	20%	67	16.0	4.0	3
12	181	124.5	21.4	7.9	32°-41°	.5-.05	33.50	1.52	12.1	2.1	17.5%	70	17.0	4.8	3
12	197	121.4	23.5	7.9	36°-44°	.5-.1	38.50	1.50	12.2	2.1	17%	68	17.0	6.0	2
12	209	124.0	24.4	8.0	39°-44°	.4-.1	38.75	1.49	12.3	2.1	17%	68	17.0	6.0	2

* M_1 = projectile mass in amu

M_2 = target mass in amu

Table 3. Rainbow scattering correlations.

Mass* M_1	M_2	E_{lab}	η	k	Fitted Region θ	σ/σ_c	θ_r (±1/2°)	r_o ±1%	R	ΔR (±12%)	$\frac{\Delta R}{R}$	ℓ_r	$\Delta\ell$	$\Delta\delta_\ell$	Reference
12	197	121.4	23.5	7.87	36°-44°	.5-.1	37.75	1.50	12.2	2.1	17%	67	17	5.7	2
14	197	145.5	27.0	9.22	36°-41°	.4-.1	36.25	1.50	12.4	2.0	16%	82	18	5.8	2
16	197	164.1	31.1	10.37	34°-41°	.7-.1	36.50	1.52	12.6	2.2	19%	94	23	7.3	2
20	197	207.6	38.6	12.87	35°-41°	.55-.1	36.75	1.47	12.5	1.9	15%	116	24	7.7	2
12	209	124.0	24.4	8.0	39°-44°	.4-.1	38.75	1.49	12.3	2.1	17%	69	17	5.7	2
14	209	145.4	28.4	9.25	39°-44°	.4-.1	39.25	1.46	12.2	1.8	15%	79	17	5.8	2
16	209	164.0	32.7	10.4	39°-44°	.34-.1	39.0	1.49	12.6	1.8	14%	92	18	6.2	2
20	209	209.6	40.3	12.96	38°-43°	.4-.1	38.75	1.44	12.5	1.7	14%	114	22	7.4	2

* M_1 = projectile mass in amu

M_2 = target mass in amu

Table 4. Comparison of values of the nuclear radius parameter, r_o, obtained from a sharp cutoff model and from rainbow model calculations.

Mass M_1	M_2	Blair r_o (fermi)	Rainbow r_o (fermi)	Reference
12	197	1.50	1.45	2
14	197	1.50	1.47	2
16	197	1.52	1.47	2
20	197	1.47	1.47	2
12	209	1.49	1.45	2
14	209	1.46	1.45	2
16	209	1.49	1.49	2
20	209	1.44	1.45	2

Table 5. Comparison of surface thicknesses computed from k and k_R.

Mass* M_1	M_2	$\Delta\ell$	k (f^{-1})	$k_R = \frac{\ell_r}{R}$ (f^{-1})	$\Delta R = \frac{\Delta\ell}{k}$	$\Delta R^* = \frac{\Delta\ell}{k_R}$	$\frac{\Delta R}{R}$	$\frac{\Delta R^*}{R} = \frac{\Delta}{\ell_r}$
14	27	2.4	2.8	1.0	.84	2.3	10%	27%
12	59	12.0	7.0	6.2	1.7	2.0	18%	21%
12	107	14.0	7.6	6.0	1.8	2.3	16.5%	22%
12	113	16.0	7.7	6.1	2.1	2.6	20%	24%
12	181	17.0	7.9	5.8	2.1	2.9	17.5%	24%
12	197	17.0	7.9	5.6	2.1	3.0	17%	25%
12	209	17.0	8.0	5.5	2.1	3.1	17%	25%

* M_1 = projectile mass in amu

M_2 = target mass in amu

Table 6. Effect of correcting for angular variation in σ/σ_c for $In^{113}(C^{12}, C^{12})In^{113}$ at E_{lab} = 124.5 Mev.

	r_o	ΔR
Uncorrected	1.53	2.14
Corrected	1.62	2.52

ORNL-3025
UC-34 - Physics and Mathematics
TID-4500 (15th ed.)

INTERNAL DISTRIBUTION

1. C. E. Center
2. Biology Library
3. Health Physics Library
4-5. Central Research Library
6. Reactor Experimental Engineering Library
7-26. Laboratory Records Department
27. Laboratory Records, ORNL R.C.
28. A. M. Weinberg
29. L. B. Emlet (K-25)
30. J. P. Murray (Y-12)
31. J. A. Swartout
32. E. H. Taylor
33. E. D. Shipley
34. S. C. Lind
35. M. L. Nelson
36. W. H. Jordan
37. C. P. Keim
38. R. S. Livingston
39. F. L. Culler
40. A. H. Snell
41. A. Hollaender
42. M. T. Kelley
43. G. E. Boyd
44. K. Z. Morgan
45. T. A. Lincoln
46. A. S. Householder
47. C. S. Harrill
48. C. E. Winters
49. H. E. Seagren
50. D. Phillips
51. R. J. Jones
52. J. J. Pinajian
53. C. D. Goodman
54. F. T. Howard
55. R. E. Worsham
56. J. A. Martin
57. P. M. Reyling
58. A. Zucker
59. J. A. Lane
60. M. J. Skinner
61. R. A. Charpie
62. R. S. Cockreham
63. W. A. Fowler (consultant)
64. H. Feshbach (consultant)
65. M. Goldhaber (consultant)
66. M. S. Livingston (consultant)
67. J. R. Richardson (consultant)
68. J. A. Wheeler (consultant)
69. J. H. Van Vleck (consultant)
70. ORNL - Y-12 Technical Library Document Reference Section

EXTERNAL DISTRIBUTION

71. Division of Research and Development, AEC, ORO
72-121. M. V. Goldman, Harvard University
122-731. Given distribution as shown in TID-4500 (15th ed.) under Physics and Mathematics category (75 copies - OTS)